A versatile control of solar DVR for enhanced utilization and power quality improvement in a series-connected wind-solar farm

Kathiresan, Aravind Chellachi; Jeyaraj, Pandia Rajan; Albert, Brindhu Kumari; Thanikanti, Sudhakar Babu; Nallapaneni, Manoj Kumar; Alhelou, Hassan Haes

Published in:
IET Renewable Power Generation

Published: 01/01/2025

Document Version:
Final Published version, also known as Publisher's PDF, Publisher's Final version or Version of Record

Published version (DOI):
10.1049/rpg2.12592

Publication details:
Kathiresan, A. C., Jeyaraj, P. R., Albert, B. K., Thanikanti, S. B., Nallapaneni, M. K., & Alhelou, H. H. (2025). A versatile control of solar DVR for enhanced utilization and power quality improvement in a series-connected wind-solar farm. *IET Renewable Power Generation*, *19*(1), Article e12592. https://doi.org/10.1049/rpg2.12592

Received: 12 January 2022 | Revised: 22 July 2022 | Accepted: 1 September 2022

DOI: 10.1049/rpg2.12592

IET Renewable Power Generation

The Institution of Engineering and Technology WILEY

ORIGINAL RESEARCH

A versatile control of solar DVR for enhanced utilization and power quality improvement in a series-connected wind-solar farm

Aravind Chellachi Kathiresan[1] | **Pandia Rajan Jeyaraj**[1] | **Brindhu Kumari Albert**[1] | **Sudhakar Babu Thanikanti**[2] | **Manoj Kumar Nallapaneni**[3] | **Hassan Haes Alhelou**[4]

[1]Department of Electrical and Electronics Engineering, Mepco Schlenk Engineering College, Sivakasi, Tamil Nadu, India

[2]Department of Electrical and Electronics Engineering, Chaitanya Bharathi Institute of Technology, Hyderabad, India

[3]School of Energy and Environment, City University of Hong Kong, Kowloon, Hong Kong

[4]Department of Electrical Power Engineering, Faculty of Mechanical and Electrical Engineering, Tishreen University, Lattakia, Syria

Correspondence
Hassan Haes Alhelou, Department of Electrical Power Engineering, Faculty of Mechanical and Electrical Engineering, Tishreen University, Lattakia 2230, Syria
Email: alhelou@ieee.org

Abstract

This paper presents a solar dynamic voltage restorer for hybrid series-connected solar-wind farms to mitigate the power quality problems. The operating region of the proposed hybrid system is derived and studied through graphical analysis. Upon examination of the system's operation under various grid conditions, the feasibility of solar PV power injected into the grid is verified. It is further proved that the series injection of voltage is also capable of mitigating the effects of voltage sag/swell, and unbalance, which have adverse effects on wind-connected induction generators. Further, the effectiveness of Solar DVR to mitigate the fault ride-through capability of the wind farm is analyzed. The non-requirement for an energy storage device such as a battery is also validated. A control system for the series PV inverter is proposed and the computer simulations are performed to confirm the efficacy and ride-through capability of the system.

1 | INTRODUCTION

Due to global environmental pollution as well as the growing energy crisis, renewable energy sources have attracted wide attention recently. Wind Energy Conversion Systems (WECS) have seen significant growth in recent years [1]. Likewise, grid integration of PV systems has also seen considerable growth, due to the decreasing cost of photovoltaic cells and recent advancements in power conversion technology and its active control [2, 3].

Owing to their complementary nature, a wind-PV hybrid generation system offers higher reliability to maintain continuous power output than any other individual power generation system [4]. Generally, hybrid system configurations exist in which PV and the wind generator are connected in parallel [5, 6], but such systems operate at high voltages, and it becomes increasingly difficult to construct PV generation systems at such high voltage levels due to several constraints. Usually, a centralized circuit, string circuit, or multi-string circuit is used for high voltage PV generation systems [7]. All of the above circuits need to connect PV modules in series to obtain a sufficient DC-link voltage for the next power conversion stage. However, it is easy for the Maximum Power Point (MPP) of the series-connected PV modules to be affected by a partial shadow which would lead to multiple power peaks and thereby cause significant mismatch losses [8]. Thus, several limitations in the parallel wind-PV hybrid configuration become evident.

Considering Wind Energy Conversion System (WECS) as an individual source, its power generation capacity is rapidly increasing, and consequently, more demanding grid standards are being implemented to wind farms, thereby guaranteeing their stability [9–10]. According to [11] and [12], two of the most significant issues that need to be addressed concerning grid integration of WECS are voltage sags and grid voltage unbalance. Shunt-based compensators such as the STATCOM [13, 14], when connected to such systems, improve the wind farm stability and regulate the voltage amplitude at the Point of Common Coupling (PCC). This mitigates the effects of voltage sags which, when present would generate transient electromagnetic torque in the generator, which results in significantly high

stresses and vibrations on the wind turbine mechanical system, having a detrimental effect on important drive-train components [15]. On the other hand, unbalanced grid voltages at the terminals of the WECS, which can be caused due to several factors, pose serious problems such as overheating, torque pulsation, and output power reduction of the induction generator [16]. The effects due to voltage sag and unbalance can be quite persistent since many wind turbines are connected to weak power systems. In such cases, steady-state voltage generally lies between +5 to −15% at the machine terminals, and unbalanced-load distributions are not corrected for many months [17].

Dynamic voltage restorers (DVRs) facilitate the control of reactive power during sags/swell, thereby enabling a quick recovery from a sudden change in the grid voltage and helping to maintain the stability of the system [18, 19]. Several configurations of STATCOMs [20–22] and DVRs [23, 24] do not analyze the performance of the compensator when unbalanced voltages arise at the PCC. However, the work in [25] can compensate for both balanced as well as unbalanced sags effectively, but it involves the combination of both a DVR and STATCOM for its operation. The DVR configuration proposed in [26] requires a battery to perform its operation, which is undesirable as it would increase the maintenance cost of the system, which is in itself costly as DVRs tend to require costly apparatus [27].

This paper introduces a hybrid wind-PV configuration where PV generation is used as the active power source instead of a battery, for a DVR in a WECS. The system in [28] where PV is used as an active power source for a DVR connected to consumer loads is capable of mitigating only mild voltage disturbances. Due to in-phase injection, harnessed power cannot be transferred to the load during healthy grid conditions and there is no active power control during voltage sags/swells. A current control topology [29] is developed to control the real and reactive power flow in a single-phase inverter from renewable energy sources

Similar work in [30] proposed a series-connected photovoltaic distributed generator that maximizes energy during daytime and enhances power quality under solar power fluctuation and voltage swell. In addition, capacitor energy storage is added to the network to enhance the power quality during insufficient solar power. A detailed numerical analysis is included in that series PV connection to identify the required capacity of the capacitor. The concept [30] is extended from voltage-sensitive loads to wind farms, but this work presents no analysis of the operating region of the series PV compensator and fails to validate the control of real and reactive power injected with it into the grid. Further, in [31], the operating region of the PV compensator is analyzed and the issue of voltage unbalance and fault ride-through capability of the wind farm has not been examined.

Thus the system proposed in this paper consists of a novel hybrid series configuration of wind and PV generator with the microgrid, and the contributions are:

(i) The system can be operated under four modes under the normal and abnormal conditions of the Grid.
(ii) The PV fed DVR is utilized more effectively using the proposed control strategy and the versatile control topology is also used to mitigate the fault ride-through capability of the wind farm
(iii) The voltage injected from PV generation being considerably lesser in magnitude (less than 40% of rated voltage), can also be used to improve the voltage quality at the terminals of the wind generator.
(iv) Without energy storage devices such as a battery, the hybrid system is capable of overcoming voltage quality issues even in the absence of solar energy (i.e. at night-time).

The system has been investigated through equations that are then graphically presented, from which the operating region of the series compensator under various disturbance conditions is studied.

The proposed system is briefly described in Section 2 and it contains a detailed analysis of its capability in PV power injection and voltage quality enhancement. The control strategy for the closed-loop operation of the PV inverter is explained in Section 3. The system behaviour under various conditions has been examined using MATLAB/Simulink and the results are presented and discussed in Section 4.

2 | SYSTEM ANALYSIS AND DESIGN CONSIDERATIONS

A schematic diagram of the system under study is shown in Figure 1a. The system consists of a 50 MW wind farm, 2.5 MW PV generator, three single-phase inverters, and a DC/DC converter. The output of Squirrel Cage Induction Generators (SCIG) based wind farm is connected in series to three single-phase inverters before its connection to the grid at the PCC. The inputs of the three single-phase inverters are connected in parallel to a common DC link. The DC-link or bus is fed from a DC–DC converter whose input is connected to a PV panel array. The three inverters inject voltages in series to fulfil the objectives of the evacuation of available PV power into the grid and maintain a balanced voltage of 1 p.u. at the terminals of the SCIG. Considering the fluctuations in the grid voltage and the available PV power, there are four possible operating modes as follows:

a. In Mode-1 (Normal operating mode) the system can able to injecting available PV power into the grid under nominal grid voltage (when the PV power is available).
b. In Mode-2 (abnormal grid with real power, P and reactive power, Q issues). The system is capable of Simultaneous sag/swell mitigation and PV power injection (marginal sag/swell in the grid voltage and PV power is available)
c. In Mode-3 the proposed system is capable of mitigating Sag/swell only, no real power injection (deep sag/ swell in grid voltage beyond mode-2) though PV power is available.
d. In Mode-4, Sag/ Swell mitigation only (when PV power is not available- Night mode)

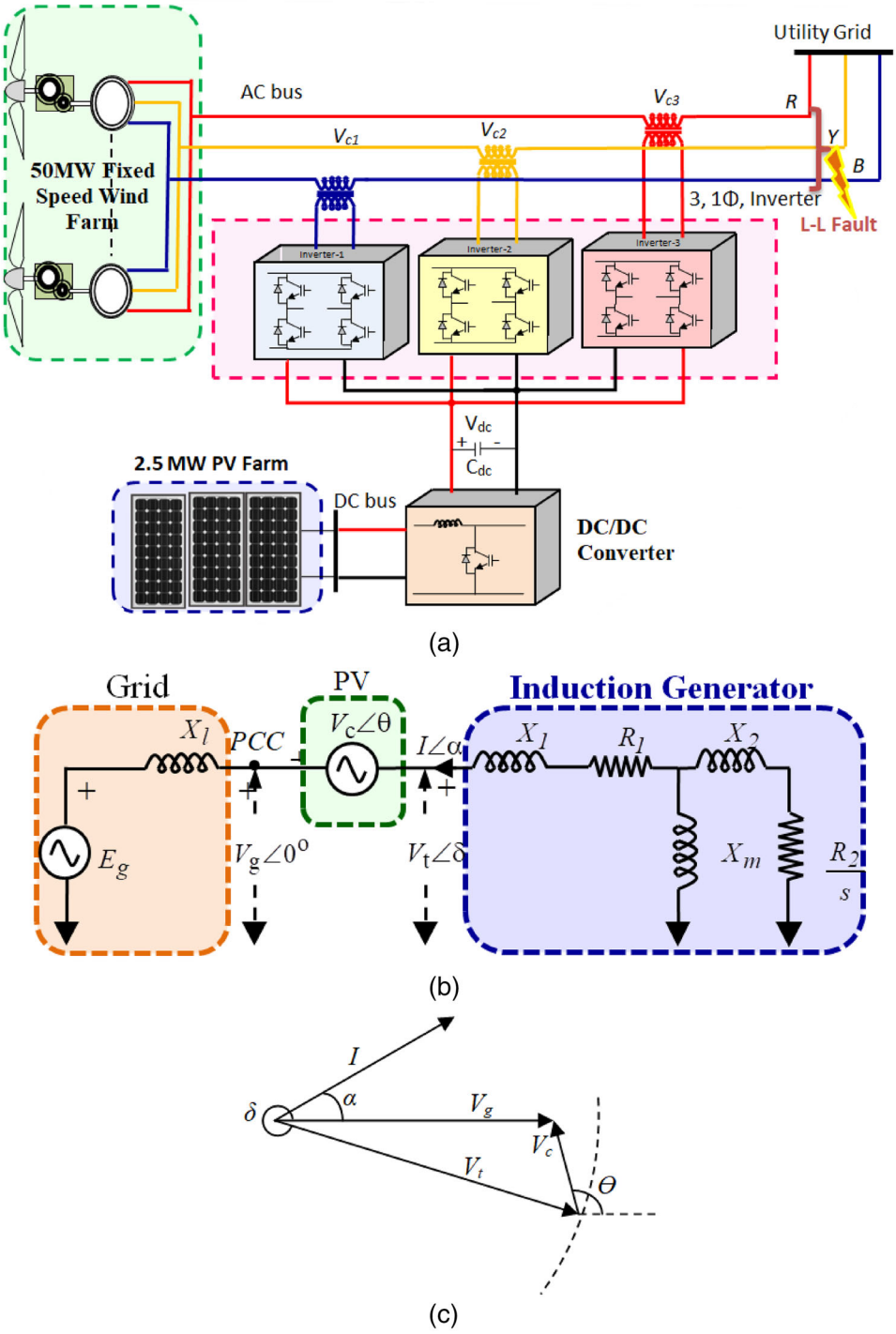

FIGURE 1 Proposed hybrid configuration: (a) Schematic of hybrid wind–PV system configuration, (b) per-phase equivalent circuit of the hybrid wind-PV system, and (c) Phasor representation of the hybrid series wind-PV system

In addition, to check the ride-through capability of the hybrid series system, a three-phase line to line fault is created at the PCC for 0.5 s. The proposed system is analyzed, both numerically and graphically based on its steady-state equations, to obtain its region of operation and presented below.

2.1 | Balanced conditions

The entire system is modelled based on the per-phase equivalent circuit (Figure 1b), initially considering a case of balanced voltage at the PCC. The source E_g signifies the grid, the voltage V_t represents the induction generator terminal

TABLE 1 Parameter of SCIG and PV

SCIG based wind farm	Parameter
Base apparent power	57.5 MVA
Rated active power	50 MW
Rated voltage (line to line)	690 V
Stator resistance (R_1)	0.0108 p.u.
Rotor resistance (R_2)	0.01214 p.u.
Mutual impedance (X_m)	4.4 p.u.
Stator impedance ($X_{1)}$	0.107 p.u.
Rotor impedance ($X_{2)}$	0.1407 p.u.
PV farm	Parameter
Rated power	2.5 MW
DC link voltage	240 V

voltage, and the voltage V_g represents the grid voltage at the PCC. It is connected to an inductance X_l, representing the inductance of the transmission line connecting the grid to the wind farm. The voltage from a PV-based inverter connected in series is represented by the voltage source V_c. The fixed speed SCIG-based wind farm is represented by its steady-state equivalent circuit. The phasor diagram of the proposed system is shown in Figure 1c. The series injection angle of voltage V_c is represented as θ, while $\angle\delta$corresponds to the terminal voltage angle. $I\angle\alpha$is the current flowing from the induction machine.

KVL equation of the system is written as:

$$V_g\angle 0° = V_c\angle\theta + V_t\angle\delta \tag{1}$$

Solving the above equation for $V_c\angle\theta$

$$|V_c| = \sqrt{\left(V_g - V_t\cos(\delta)\right)^2 + \left(V_t\sin(\delta)\right)^2} \tag{2}$$

$$\theta = \tan^{-1}\left(\frac{V_t\sin(\delta)}{V_t\cos(\delta) - V_g}\right) \tag{3}$$

The real power (P_c) and reactive power (Q_c) injected by the compensator are given by:

$$P_c = \frac{V_t^2}{Z}\cos\varphi - \frac{V_gV_t}{Z}\cos(\varphi - \delta) \tag{4}$$

$$Q_c = \frac{V_t^2}{Z}\sin\varphi - \frac{V_gV_t}{Z}\sin(\varphi - \delta) \tag{5}$$

where$Z\angle\varphi$ is the equivalent impedance of the induction machine at a specific value of slip. From (4) and (5) eliminating δ,

$$\left(P_c - \frac{V_t^2}{Z}\cos\varphi\right)^2 + \left(Q_c - \frac{V_t^2}{Z}\sin\varphi\right)^2 = \left(\frac{V_gV_t}{Z}\right)^2 \tag{6}$$

From (6), it can be seen that the P_c versus Q_c graph consists of concentric circles shifted from the origin, for various conditions of grid voltage V_g. For the purpose of graphical analysis, a practical system is considered whose p.u. ratings are as shown in Table 1. By using the above rating, the operating region is plotted for different voltages at the PCC.

The graph in Figure 2a shows concentric circles for different operating grid voltages V_{g1}-V_{g6}, whose centre is shifted from the origin. The centre of these circles (point E) corresponds to the ($\frac{V_t^2}{Z}\cos\varphi$, $\frac{V_t^2}{Z}\sin\varphi$)which represents the real and reactive power injected by the wind generator at a given slip when the grid voltage is zero, but a voltage of 1 p.u. is maintained at the machine terminals by the series compensator. Thus, at point E it is evident that the compensator has to absorb the active power produced by the wind generator, in order to maintain a constant voltage of 1 p.u. at terminals of the SCIG. The centre lying on the negative X-axis implies that real power is absorbed by the compensator, rather than real power being supplied from it. Also, a positive Q_C indicates that the compensator delivers reactive power to the generator. Figure 2a represents an analysis of the system under full load slip ($s_{fl} = -0.0135$), while Figure 2b represents the case of a lower *slip* ($s_1 = -0.01$). The radius of these circles represents the grid voltage magnitude in p.u. These graphs are valid for any series compensator connected to this SCIG-based Windfarm. Each point on the circles corresponds to a particular value of injected voltage, resulting

in real and reactive power flow from the series compensator such that the terminal voltage of the SCIG is maintained at 1 p.u. during grid voltage sags/swells. In comparison, the graph in Figure 2b has a smaller radius and is shifted towards the positive real axis, since the machine is operated at a lower value of slip. It can be deduced that at a higher value of slip, as the amount of wind power generated increases for a particular grid voltage, the amount of PV power that can be injected in series also marginally increases.

Likewise, the circles with their centres at the origin show the constraint on the magnitude of the series injected voltage. The radius of these circles represents the magnitude of voltage injected in series. The proposed series PV-based inverter will have a given V_{cmax}, and since the use of an energy storage device is avoided, the region in the negative X-axis is not part of the operating region. Therefore the effective operating region of the inverter with $V_{cmax} = 0.4$ p.u. is the shaded region in the graph. For further examination of the system, a graph is plotted showing the shaded region in Figure 2a alone in greater detail, in Figure 2c. The operation of the system during voltage sags and swells is described in Figure 2c, from which the power rating of the PV system for MPPT can also be obtained, which is subsequently explained.

For understanding the operation of the system, a typical case where available PV power is P_x and grid voltage is 1 p.u is considered. This operating point, which on the curve representing V_{g3}, is shown as point A in Figure 2c. Now if there is a grid voltage sag of 0.05 p.u. or swell of 0.05 p.u. the operating point will shift to points B or C respectively, assuming PV power remains constant. Now if the system is operating at point A, and PV

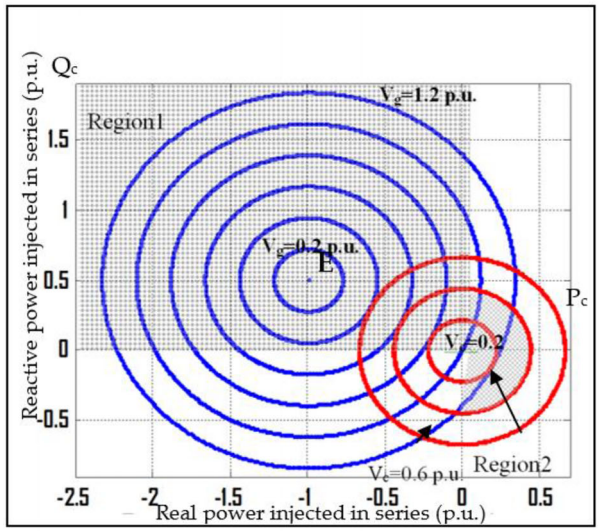

FIGURE 2 Operating region of series compensator $V_{g1} < V_{g6}$: (a) With rated slip, (b) with low rated slip, and (c) magnified view of operating region at rated slip, $V_{g1} < V_{g10}$

power decreases to zero with constant grid voltage, then the operating point will travel along the curve corresponding to 1 p.u. which V_{g3}, to point D. In order to achieve MPPT under grid voltages above 0.95 p.u., it is graphically depicted by a straight line, which is drawn from the curve V_{g2} and cuts the X-axis at 0.06 p.u., thus showing that a PV system of this particular value of power rating ought to be chosen. This value is further validated by numerical analysis which follows. From this investigation, it is deduced that operation below a minimum voltage sag level will not be possible unless an Energy Storage Device such as a battery is incorporated.

$$\delta_{night} = \varphi - \cos^{-1}\left(\frac{V_t}{V_g}\right)\cos\delta \tag{7}$$

$$Q_{c\,night} = \frac{V_t^2}{Z}\sin\varphi - \frac{V_g V_t}{Z}\sin\left(\varphi - \delta_{night}\right) \tag{8}$$

During night-time operation, when PV power is zero, (7) and (8) can be used to determine the operating value of 'δ' and the amount of reactive power absorbed or injected by the series compensator.

$$P_{PV\,(rated)} = \frac{V_t^2}{Z_1}\cos\varphi - \frac{V_{g\min} V_t}{Z_1}\cos\left(\varphi - \delta_1\right) \tag{9}$$

where,

$$\delta_1 = \cos^{-1}\left(\left(\frac{V_{g\min}}{2V_t}\right) + \left(\frac{V_t}{2V_{g\min}}\right) - \left(\frac{V_{c\max}^2}{2V_{g\min}V_t}\right)\right) \tag{10}$$

$$V_{g\min} = \frac{V_t\cos\varphi}{\cos\left(\varphi - \delta\right)} - \frac{ZP_{PV}}{V_t\cos\left(\varphi - \delta\right)} \tag{11}$$

When determining the rating of the PV panels to be installed, according to (9) and (10), it is vital to know V_{gmin} so that MPPT can be implemented under all conditions. V_{gmin} is the minimum steady-state grid voltage recorded at the terminals of the generator, which needs to be restored. Hence rated PV Power can be obtained. Moreover using (11), one can also obtain the maximum voltage dip which can be compensated by a specific rating of PV farm operating with MPPT.

For a case of $V_{gmin} = 0.95$, a value adopted from [10], Equations (9) and (10) are numerically solved by substituting the machine parameters when it operates at its full load slip. The value of the PV power rating obtained is 0.061 p.u. which substantiates the value obtained by graphical analysis. From Figure 2c, it is clear that higher values of V_{gmin} enable the installation of PV with higher ratings.

2.2 | Unbalanced conditions

In the previous section, the operating point in the P_c versus Q_c graph (Figure 2a) was chosen based on the grid voltage and the amount of PV power available. Due to its independent occurrence in each phase, an issue arises in certain cases when the

grid voltage in each phase differs. This leads to the issue of having a different δ for each phase, which contributes to the loss of the 120° phase difference between each phase. Therefore, a control strategy to overcome this issue is devised, so as to divide the available PV power among the three phases while maintaining the same δ, so that a 120 ° phase shift between the three phases is always maintained.

Let P_{PV} be the average power injected per phase,

$$P_{c1} + P_{c2} + P_{c3} = 3P_{PV} \tag{12}$$

where P_{c1}, P_{c2}, P_{c3} are the powers injected in each phase of the DVR. Using (4) in (12), we get,

$$3k_1 + \left(V_{g1} + V_{g2} + V_{g3}\right) k_2 = 3P_{PV} \tag{13}$$

where$k_1 = (\frac{V_t^2}{Z}\cos\varphi)$,$k_2 = (\frac{V_t}{Z}\cos(\varphi - \delta))$, k_2' can be found yielding δ (same for all phases). Using (4) the power injected in each phase can be found. Also, after obtaining δ from the above method, $V_c\angle\theta$ each of the three phases of the Series PV generator use can be obtained from (2) and (3). Operating at the δ obtained above ensures both, the pumping of available PV power at any instant as well as the removal of any unbalance in the voltage at the terminal of the induction generator.

3 | CONTROL SCHEME

3.1 | Inverter control strategy

Conventional DVR (Inverter) operates only under abnormal conditions, that is, whenever any abnormalities occur in the grid, then the inverter injects the required amount of power to maintain stability. But, in normal grid conditions, this inverter is in idle mode. This shows that the utilization factor of the conventional inverter is very less.

In the proposed Solar Dynamic Voltage Restorer, the utilization factor of the inverter is increased by using the proposed effective control topology. During abnormal conditions, the inverter compensates for the abnormalities and during the normal operating condition, the inverter injects the generated PV power into the grid. Figure 3 Shows the Proposed Control Strategy for a Solar DVR.

During closed-loop operation of the system, the three single-phase inverters need to inject voltages such that PV power is evacuated and voltage sags/swells are eliminated. The linear relationship between power injected and δ is identified and used for the operation of the inverters. Equation (4) shows this relationship, which is considered linear for small values of δ. Therefore, a PI controller is used for the DC bus Voltage control [32]. The capacitor voltage at the DC bus and reference DC voltage are used as inputs to obtain the operating value of δ. This value is used to generate the reference waves for the three single-phase inverters. A double loop control using PI compensators is employed for effective and dynamic control of the inverters. Since the inverter current is the fastest-changing parameter, the inner loop involves current control, and voltage is controlled in the outer loop. Feed-forward Phase Locked Loop-based synchronization is implemented to reduce the tracking time [33, 34]. The control schemes are integrated to form the overall control system shown in Figure 3

Table 2 shows the effective utilization of Solar DVR in a hybrid Series Wind-PV system under all operating conditions.

The energy extracted from the PVDVR and the FSWG system is calculated based on the average capacity factor of the solar PV power generation system and wind generation system.

The average capacity factor of solar PV system is 28% as reported in International Renewable Energy Agency (IRENA) in the year of 2017 and thus the energy extraction from PVDVR is given as follows:

$$\text{Energy extracted/year} = P_{PV\text{-}rating} \times CF_{PV} \times T \tag{14}$$

where $P_{PV\text{-}rating}$ is the installed capacity of PV system, CF is the Capacity Factor of solar PV and T denotes total hours in a year.

The average capacity factor of wind generation system is approximately 34.5% as reported in International Renewable Energy Agency (IRENA) in the year of 2017 and thus the energy extraction from FSWG system is given as follows:

$$\text{Energy extracted/year} = PWF\text{-}rating \times CF_{WG} \times T \tag{15}$$

where *PWF-rating* is the installed capacity of FSWG system, CF_{WG} is the capacity factor of wind generation system and T is the total hours in a year.

The total energy extracted from FSWG system is calculated as 153300 MWh/year using (15). With the addition of PVDVR in FSWG system, the energy extracted is 14716.8 MWh. Therefore, the percentage increase in the energy extraction in the FSWG system with addition of PV system in the DVR is approximately 10% and thus the total energy extracted from the FSWG and PVDVR is 168016.5 MWh. Therefore, addition of PV system in DVR improves the utilization of DVR by extracting energy from PV system instead of keeping the DVR idle under nominal grid voltage condition.

4 | RESULTS AND DISCUSSION

A 2.5 MW PV generator connected in series to a 50 MW Wind Farm with the mentioned above specifications is simulated in MATLAB Simulink and the effectiveness of the proposed system is verified under various operating conditions of the grid voltage and available PV power.

4.1 | Step-change in PV power under ideal grid conditions

Considering a nominal grid voltage, and the available PV power to be 0.02 p.u., the operating point is 'B' in region R_2 as shown in Figure 2. The output response of the system is shown in Figures 4 and 5. The figure depicts the behaviour of the system when there is a change in the amount of sunlight falling on

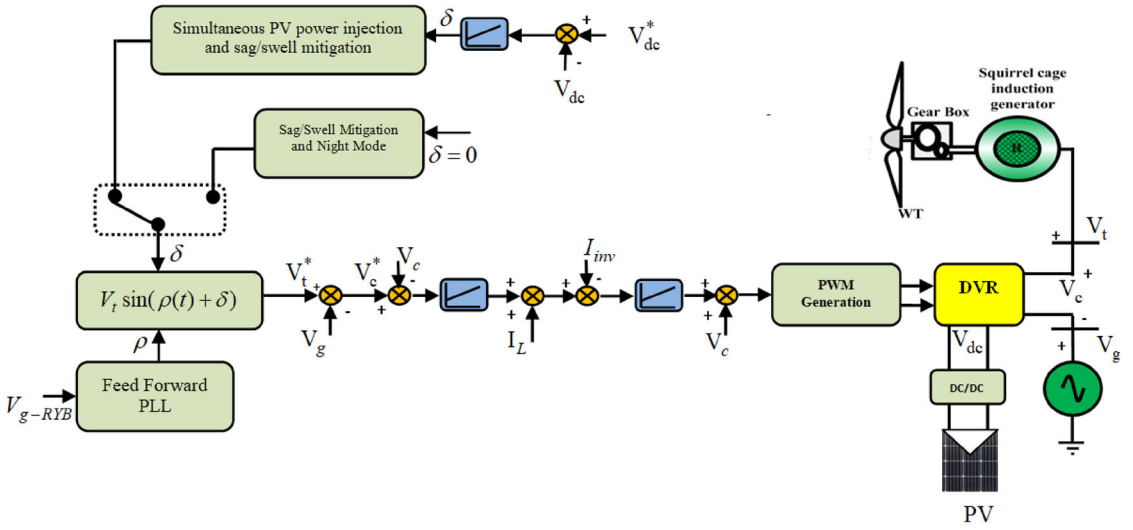

FIGURE 3 Proposed control strategy for hybrid series wind-solar system

TABLE 2 Real and reactive power exchange under various mode

Grid conditions	DVR with capacitor	DVR with energy storage	PV DVR (proposed)
Under steady state condition and PV power is available	Idle	Idle	Inject available PV power into grid
Under marginal sag/swell in the grid voltage and PV power is available	Sag/swell mitigation only	Sag/swell mitigation and inject real power for short period (based on the available energy storage)	Sag/swell mitigation and inject available PV Power into the grid
Under deep sag/swell in the grid voltage and PV power is available	Sag/swell mitigation only	sag/swell mitigation	Sag/swell mitigation Ooly
Sag/swell when PV power is not available	Sag/swell mitigation only	Sag/swell mitigation	Sag/swell mitigation
Under fault condition	Idle	Idle	inject reactive power into wind farm

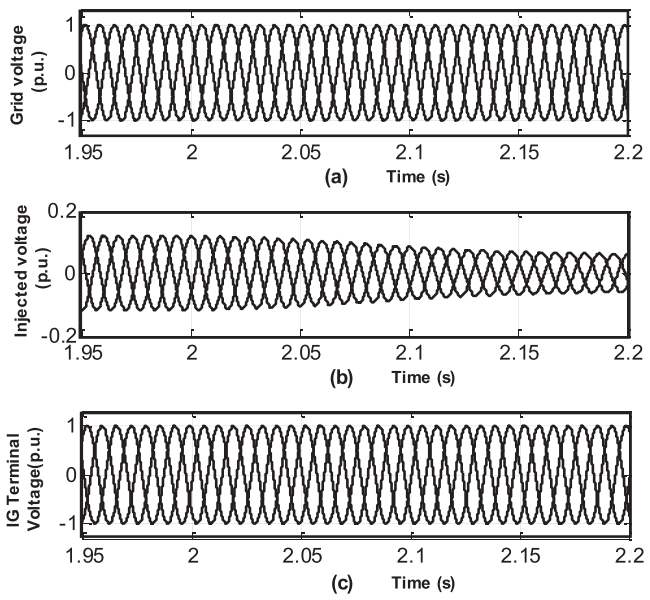

FIGURE 4 System voltage response under ramp change in PV power: (a) Grid voltage, (b) injected voltage, and (c) IG terminal voltage

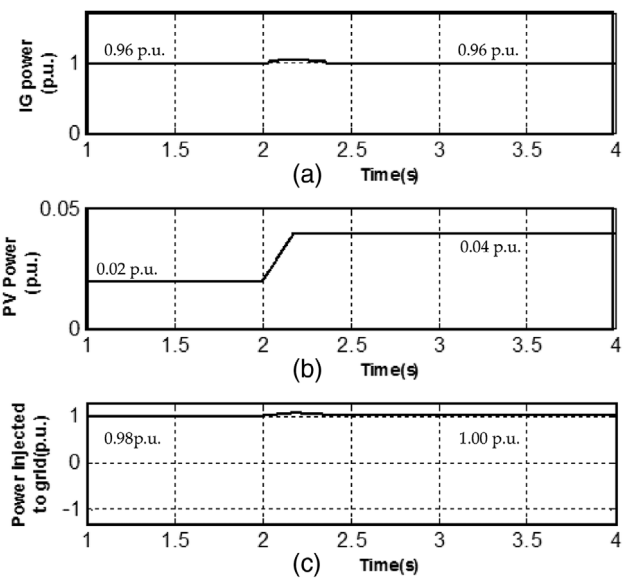

FIGURE 5 Response of system power under ramp change in PV power: (a) IG power, (b) PV power, and (c) total power injected into the grid

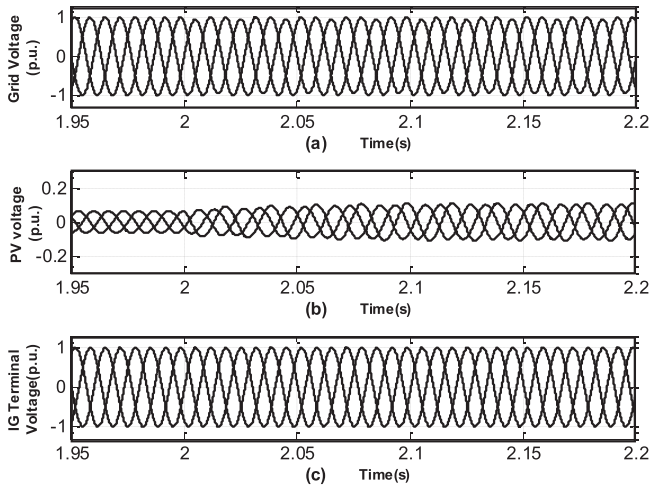

FIGURE 6 System response for unsymmetrical voltage sags of 0.05 p.u. ($V_R = 0.95$, $V_Y = 1$, $V_B = 1$): (a) Grid voltage, (b) injected voltage, and (c) IG terminal voltage

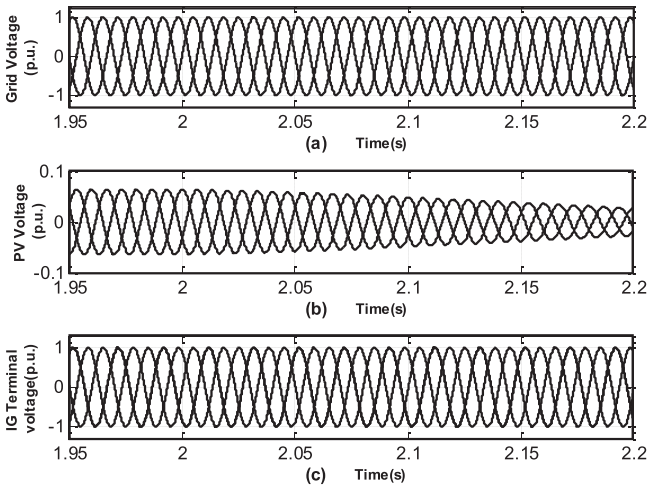

FIGURE 8 System voltage response under night mode operation with unsymmetrical voltage sag: (a) Grid voltage, (b) injected voltage, and (c) IG terminal voltage

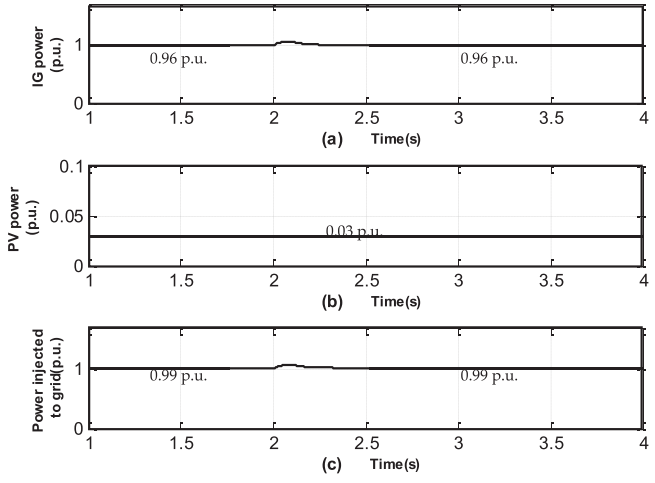

FIGURE 7 Response of system power for unsymmetrical voltage sags of 0.05 p.u: (a) IG power, (b) PV power, and (c) total power injected into the grid

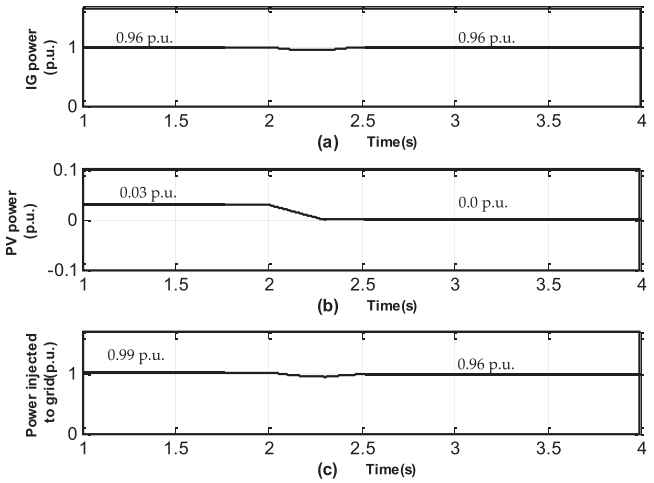

FIGURE 9 System voltage response under night mode operation with unsymmetrical voltage sag: (a) IG power, (b) PV power, and (c) total power injected into the grid

the PV farm. At $t = 0.2$ s the irradiation of the PV is increased which increases by injecting PV power from an initial value of 0.02–0.04 p.u. In this case, even though the PV output power changes, a balanced voltage of 1 p.u. is maintained across each phase of the SCIG by the PV-based compensator.

4.2 | Introduction of unsymmetrical voltage sag at the PCC under constant solar irradiation

In the case of an unsymmetrical sag in grid voltage with an available PV power of 0.03 p.u., a 10% of sag is introduced at $t = 2$ s in one phase (R) of grid voltage. and Y and B phases are maintained with the nominal grid voltage.

The graphs in Figures 6 and 7 depict the behaviour of the system when an unbalanced voltage sag is introduced at the PCC. Initially, there is a symmetrical sag of 0.98 p.u. and at 't = 2 s, a further sag of 0.95 p.u. is introduced in one of the phases. The PV power remains constant throughout at the value of 2 MW. The compensator acts in each phase individually and hence mitigates the unbalance at the terminals of the machine.

5 | INTRODUCTION OF UNSYMMETRICAL VOLTAGE SAG AT THE PCC UNDER NIGHTTIME CONDITIONS

Whenever PV power is not available, DVR is operated in Mode-4 for the only sag/swell mitigation. The graphs in Figures 8 and 9 depict the behaviour of the system when an unbalanced voltage sag is introduced at the PCC. Since night-time conditions are simulated, PV power is zero. Initially conditions of 0.99 p.u. symmetrical sag exists, while at 't = 2 s, an unbalance arises

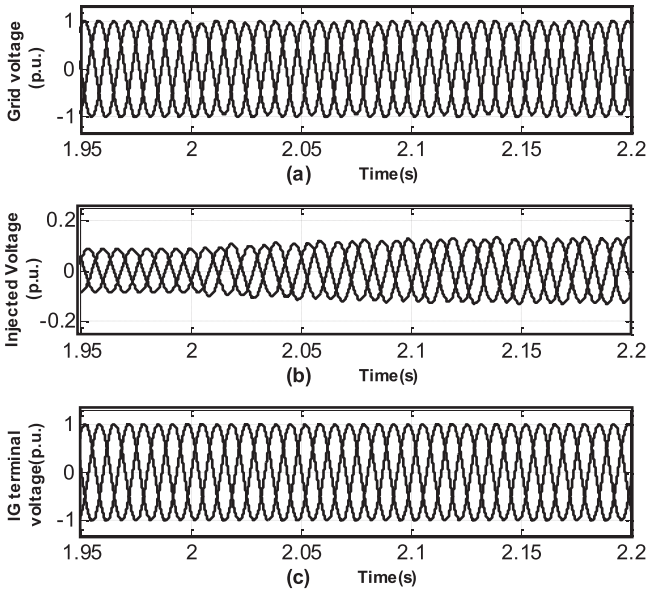

FIGURE 10 Voltage response for change in wind speed: (a) Grid voltage, (b) injected voltage, and (c) IG terminal voltage

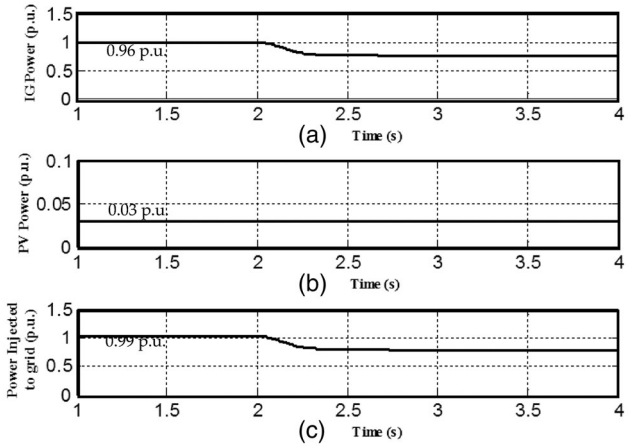

FIGURE 11 Response of system power for change in wind speed: (a) IG power, (b) PV power, and (c) total power injected into the grid

in one of the phases. The performance of the system is found to be satisfactory even during night-time operation.

5.1 | Step-change in wind speed

The graphs in Figures 10 and 11 represent the behaviour of the system when there is a change in wind speed causing the operating slip to dip from 1.0135 to 1.01 p.u. The compensator can perform its function before and after the change in mechanical power input to the generator. The result shows the performance of the proposed scheme under varying grid voltage and PV power

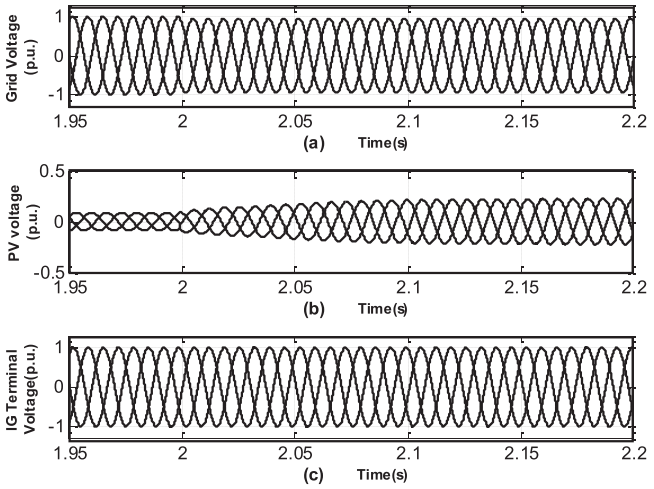

FIGURE 12 System response for symmetrical voltage sags of 0.05 p.u. ($V_R = 0.95$, $V_Y = 0.95$, $V_B = 0.95$): (a) Grid voltage, (b) injected voltage (c) IG terminal voltage

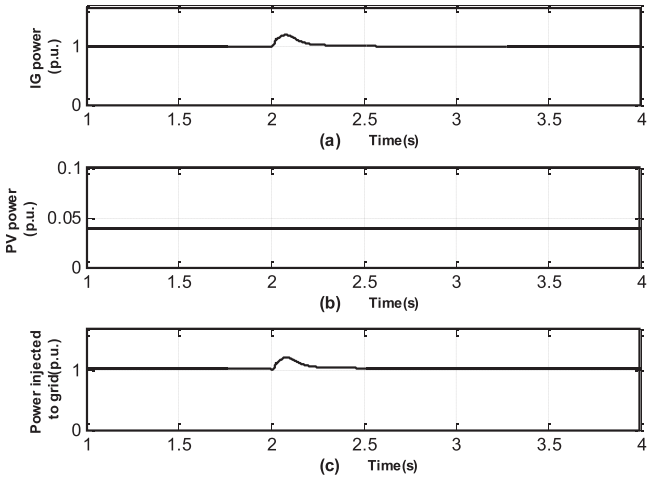

FIGURE 13 Response of system power for symmetrical voltage sag: (a) IG power, (b) PV power, and (c) total power injected into the grid

5.2 | Introduction of symmetrical voltage sag at the PCC under constant solar irradiation

The graphs in Figures 12 and 13 depict the behaviour of the system when a balanced voltage sag is introduced at the PCC. Asymmetrical voltage sag of 0.05 p.u. is introduced at time $t = 2$ s and the PV power remains constant at a value of 0.04 p.u. Instantly the controller generates the control pulse to inject a compensation voltage from the PV fed three, single-phase inverters to mitigate the voltage sag and maintain the constant voltage of 1 p.u. at the machine terminals. From these analyses, it is observed that the proposed system effectively works under various grid conditions and the series injection of voltage is also capable of mitigating the effects of voltage sag/swell and unbalance, which have adverse effects on wind connected induction generators.

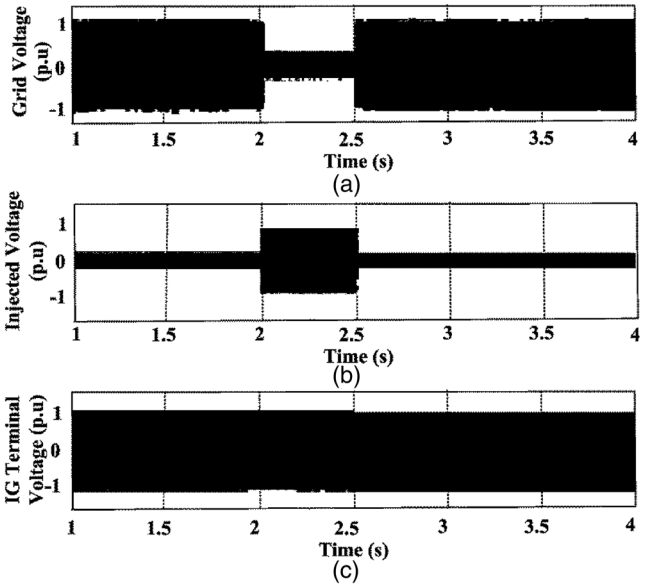

FIGURE 14 System response for line to line fault with a voltage sag of 64% ($V_R = 0.36$, $V_Y = 0.36$, $V_B = 0.36$): (a) Grid voltage, (b) injected voltage (c) IG terminal voltage

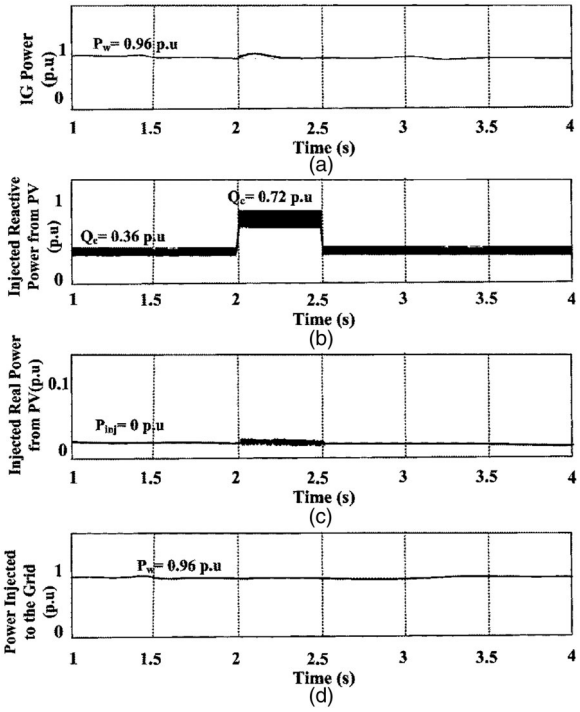

FIGURE 15 Response of system power under L–L fault: (a) IG power, (b) injected reactive power from PV fed Inverter, (c) injected real power from PV fed inverter, and (d) total power injected into the grid

5.3 | Fault ride-through capability of a hybrid series wind PV system

To verify the fault ride-through capability of the hybrid system, a symmetrical fault with fault impedance of 1.16 ohms is applied at the grid for a duration of 0.5 s at time $t = 2$ s for the following pre-fault conditions.

a. The wind generator operates at rated wind speed and it is generating 48 MW of power
b. The solar power is operated under night mode (Mode-4).

The contribution of PV-fed DVR to the fault ride-through capability of the wind farm is analyzed using Matlab simulation. To validate the behaviour of the system, the wind farm is operated near its rated capacity of 0.96 p.u. During the fault ride-through capability test, a three-phase line to line fault is created near the utility grid for 0.5 s and the response of the system is shown in Figures 14 and 15. The fault in the system creates a voltage sag of 0.64 p.u. at the PCC for 0.5 s (shown in Figure 15a. Before fault, the wind generator generates 0.96 p.u. real power by absorbing 0.36 p.u. reactive power from the PV fed inverter. During the fault, the versatile controller controls the PV fed inverter to inject 0.72 p.u. reactive power with zero real power to PCC to compensate for the grid voltage (shown in Figure 15b,c). Figure 14c shows the stabilized voltage of 1 p.u. the voltage across the PCC which is injected by the PV-based compensator.

During this case, the PV power is not available (night mode), and the hybrid system operates in mode-4 to mitigate the voltage sag generated due to a three-phase L–L fault. The compensated real and reactive power during this operation is calculated using (7) and (8). Figure 15a,d represents the generated IG Power that is injected at the utility grid. From this fault ride-through capability analysis, it is noted that a PV-based compensator improves the operation of the wind farm during any abnormal conditions.

6 | CONCLUSIONS

This paper examines the feasibility of a hybrid system involving the injection of PV power in series with a wind-driven SCIG farm. In addition to having the function of maximizing solar energy harnessed from the PV panels and feeding it to the grid, the PV-based series device also improves the voltage quality at the terminals of the SCIG. Thereby, the adverse effects caused by line-to-line fault, voltage sags/swells, and unbalance at the terminals of the induction generator are mitigated. The system is capable of smooth operation even during night-time, that is, when solar energy is absent. The PVDVR increases the utilization of inverter by injecting real power to the grid under Idle mode. From the result section, it can be found to be favourable without the need for an energy storage device such as a battery, provided the grid voltage is above a minimum threshold.

The analysis performed and presented in this work is supported by an extensive series of simulations for various conditions. The simulation and results demonstrate that the injection of PV power in series through a compensating device to SCIG-based wind farms, performs as predicted by the analytical model in enhancing the voltage quality, thus forming a very efficient wind-PV hybrid configuration.

ACKNOWLEDGEMENTS

The authors thank the Department of Electrical and Electronics Engineering, Mepco Schlenk Engineering College, Sivakasi, India for providing us with the necessary research facilities to carry out this work. This research work is supported by the Department of Science and Technology, Science and Engineering Research Board (DST-SERB) project under the Teachers Associateship for Research Excellence (TARE) scheme TAR/2021/000396.

FUNDING INFORMATION

The authors received no funding for this work.

CONFLICT OF INTEREST

There is no conflict of interest.

DATA AVAILABILITY STATEMENT

Data sharing is not applicable to this article as no new data were created or analyzed in this study.

ORCID

Aravind Chellachi Kathiresan https://orcid.org/0000-0002-3231-2637
Pandia Rajan Jeyaraj https://orcid.org/0000-0001-7086-6596
Sudhakar Babu Thanikanti https://orcid.org/0000-0003-0737-3961
Hassan Haes Alhelou https://orcid.org/0000-0001-8176-1589

REFERENCES

1. The Global Wind Energy Council, *GWEC's Global Wind Report*, (2019)
2. International Energy Agency Photovoltaic Power Systems, IEA PVPS(2012). Trends in photovoltaic applications. Survey report of selected IEA countries between 1992 and 2011. Int. Energy Agency Photovoltaic Power Syst. (IEA PVPS), (2012)
3. Fang, Z., Lin, Y., Song, S., Li, C., Lin, X., Chen, Y.: State estimation for situational awareness of active distribution system with photovoltaic power plants. In: IEEE Trans. Smart Grid. 12(1), 239–250 (2021)
4. Sarkar, S., Ajjarapu, V.: MW resource assessment model for a hybrid energy conversion system with wind and solar resources. IEEE Trans. Sustainable Energy. 2(4), 383–39 (2011)
5. Gupta, T.N., Murshid, S., Singh, B.: Power quality improvement of single phase weak grid interfaced hybrid solar PV and wind system using double fundamental signal extracter-based control. IET Gener. Transm. Distrib. 13(17), 3988–3998 (2019)
6. Lin, S., Wang, Y., Liu, M., Fan, G., Yang, Z., Li, Q.: Stochastic optimal dispatch of PV/wind/diesel/battery microgrids using state-space approximate dynamic programming. IET Gener. Transm. Distrib. 13(15), 3409–3420 (2019)
7. Wanik, M.Z.C., Jabbar, A.A., Singh, N.K., Sanfilippo, A.P.: Comparison on the impact of 0.4 MW PV with central inverter vs string inverter on distribution network operation. In: *IEEE 7th International Conference on Power and Energy (PECon)*, Kuala Lumpur, Malaysia, pp. 162–167 (2018)
8. Teo, J.C., Tan, R.H.G., Mok, V.H., Ramachandaramurthy, V.K., Tan, C.: Impact of partial shading on the P–V characteristics and the maximum power of a photovoltaic string. Energies 11, 1860 (2018)
9. Altin, M., Goksu, O., Teodorescu, R., Rodriguez, P., Jensen, B.B., Helle, L.: Overview of recent grid codes for wind power integration. In: *12th International Conference on Optimization Electrical and Electronic Equipments (OPTIM)*, Brasov, Romania, pp. 1152–1160 (2010)
10. Jeyaraj, P.R., Kathiresan, A.C., Asokan, S.P., Nadar, E.R.S., Rezk, H., et al.: Power system resiliency and wide area control employing deep learning algorithm. Comput. Mater. Contin. 68(1), 553–567 (2021)
11. Chen, Z.: Issues of connecting wind farms into power systems. In: *Transmission and Distribution Conference and Exhibition: Asia and Pacific*, Dalian, China, pp.1–6 (2005)
12. Ray, P.K., Mohanty, S.R., Kishor, N.: Classification of power quality disturbances due to environmental characteristics in distributed generation system. IEEE Trans. Sustainable Energy 4(2), 302–313 (2013)
13. Aten, M., Martinez, J., Cartwright, P.J.: Fault recovery of a wind farm with fixed-speed induction generators using a STATCOM. Wind Eng. 29(4), 365–375 (2005)
14. Xueguang, W., Atputharajah, A., Changjiang, Z., Jenkins, N.: Application of a static reactive power compensator (STATCOM) and a dynamic braking resistor (DBR) for the stability enhancement of a large wind farm. Wind Eng. 27(2), 93–106 (2003)
15. Badrinath, V., Santos-Martin, D., Jensen, H.M.: Voltage sag influence on fatigue life of the drivetrain of fixed speed wind turbines. J. Eng. Appl. Sci. 6(3) 106–115 (2011)
16. Muljadi, E., Yildirim, D., Batan, T., Butterfield, C.P.: Understanding the unbalanced-voltage problem in wind turbine generation. Ind. Appl. Conf. 2(1), 1359–1365 (1999)
17. Sorensen, P., Hauge Madsen, P., Vikkelso, A., Kolbak Jensen, K., Fathima, K.A., Unnikrishnan, A.K.: Power quality and integration of wind farms in weak grids in India. In: *Report of RISOE National Laboratory Roskilde*, Denmark (2000)
18. Jayaprakash, P., Singh, B., Kothari, D.P.: Current mode control of Dynamic Voltage restorer for power quality improvement in distribution system. In: 2008 IEEE 2nd International Power and Energy Conference, Johor Bahru, Malaysia, pp. 301–306 (2008)
19. Jayaprakash, P., Singh, B., Kothari, D.P., Chandra, A., Al-Haddad, K.: Control of reduced-rating dynamic voltage restorer with a battery energy storage system. IEEE Trans. Ind. Appl. 50(2), 1295–1303 (2014)
20. Chellachi Kathiresan, A., Ilango, G.S., Nagamani, C., Reddy, M.J.B.: A control strategy for hybrid autonomous power system with a battery management scheme. Electr. Power Compon. Syst. 43(8–10), 1159–1172 (2014)
21. Aravind, C.K., Saravana Ilango, G., Nagamani, C.: A smooth co-ordination control for a hybrid autonomous power system (HAPS) with battery energy storage (BES). Front. Energy. 9, 31–42 (2015)
22. Nasiri, M.R., Farhangi, ;S., Rodríguez, J.: Model predictive control of a multilevel CHB STATCOM in wind farm application using diophantine equations. IEEE Trans. Ind. Electron. 66(2), 1213–1223 (2019)
23. Gaztanaga, H., Etxeberria-Otadui, I., Bacha, S., Roye, D.: Fixed-speed wind farm operation improvement by using DVR devices. In: IEEE International Symposium on Industrial Electronics, Vigo, Spain, pp. 2679–2684 (2007)
24. Ye, J., Gooi, H.B.: Phase angle control based three-phase DVR with power factor correction at point of common coupling. J. Mod. Power Syst. Clean Energy 8(1), 179–186 (2020)
25. Leon, A.E., Farias, M.F., Battaiotto, P.E., Solsona, J.A., Valla, M.I.: Control strategy of a DVR to improve stability in wind farms using squirrel-cage induction generators. IEEE Trans. Power Syst. 26(3), 1609–1617 (2011)
26. Ramachandaramurthy, V.K., Fitzer, C., Arulampalam, A., Zhan, C.: Control of a battery supported dynamic voltage restorer. IEE Proc. Gener. Transm. Distrib. 149(5), 533–542 (2002)
27. Woodley, N.H.: Field experience with dynamic voltage restorer (DVRT-MMV) systems. IEEE Power Eng. Soc. Winter Meet. 4, 2864–2871 (2000)
28. Kong, F., Rodriguez, C., Amaratunga, G., Panda , S.K.: Series connected photovoltaic power inverter. In: International Conference on Electrical Machines and Systems (ICEMS), Busan, Korea (South), pp. 595–600 (2008)
29. Dasgupta, S., Sahoo, S.K., Panda, S.K., et al.: Single-phase inverter-control techniques for interfacing renewable energy sources with microgrid-part II: Series-connected inverter topology to mitigate voltage-related problems

along with active power flow control. IEEE Trans. Power Electron. 26(3), 732–746 (2011)
30. Saadat, N., Choi, S.S., MahindaVilathgamuwa, D.: A series-connected photovoltaic distributed generator capable of enhancing power quality. IEEE Trans. Energy Conserv. 28(4), 1026–1035 (2013)
31. Priyavarthini, S., et al.: Pv-fed DVR for simultaneous real power injection and sag/swell mitigation in a wind farm. IET Power Electron. 11(14), 2385–2395(2018)
32. Kjaer, S., Pedersen, J., Blaabjerg, F.: A review of single-phase grid connected inverters for photovoltaic modules. IEEE Trans. Ind. Appl. 41(5), 1292–1306 (2005)
33. Kathiresan, A.C., PandiaRajan, J., Sivaprakash, A., Sudhakar Babu, T., Islam, M.R.: An adaptive feed-forward phase locked loop for grid synchronization of renewable energy systems under wide frequency deviations. Sustainability 12, 7048 (2020)
34. Dionisio, R., Sergio, M., Carlos, A., Francisco, B., Rosa, M.C.: Low-voltage ride-through capability for wind generators based on dynamic voltage restorers. IEEE Trans. Energy Convers. 26, 195–203 (2011)

How to cite this article: Kathiresan, A.C., Jeyaraj, P.R., Albert, B.K., Thanikanti, S.B., Nallapaneni, M.K., Alhelou, H.H.: A versatile control of solar DVR for enhanced utilization and power quality improvement in a series-connected wind-solar farm. IET Renew. Power Gener. 19, e12592 (2025).
https://doi.org/10.1049/rpg2.12592